

Josephson current in an irradiated Weyl semimetal junction

Han Wang(王含) and Rui Shen(沈瑞)

Citation: Chin. Phys. B, 2021, 30 (**7**): 077406. DOI: 10.1088/1674-1056/ac0348
Journal homepage: http://cpb.iphy.ac.cn; http://iopscience.iop.org/cpb

What follows is a list of articles you may be interested in

Anomalous Josephson current in quantum anomalous Hall insulator-based superconducting junctions with a domain wall structure

Qing Yan(闫青), Yan-Feng Zhou(周彦峰), Qing-Feng Sun(孙庆丰)
Chin. Phys. B, 2020, 29 (**9**): 097401. DOI: 10.1088/1674-1056/aba272

Quadruple-stacked Nb/Nb_xSi_{1-x}/Nb Josephson junctions for large-scale array application

Wenhui Cao(曹文会), Jinjin Li(李劲劲), Lanruo Wang(王兰若), Yuan Zhong(钟源), Qing Zhong(钟青)
Chin. Phys. B, 2020, 29 (**6**): 067404. DOI: 10.1088/1674-1056/ab90e3

Giant enhancement of superconductivity in few layers $MoTe_2$

Yuan Gan(甘远), Chang-Woo Cho, Alei Li(李阿蕾), Jian Lyu(吕坚), Xu Du(杜序), Jin-Sheng Wen(温锦生), Li-Yuan Zhang(张立源)
Chin. Phys. B, 2019, 28 (**11**): 117401. DOI: 10.1088/1674-1056/ab457f

Josephson effect in the strontium titanate/lanthanum aluminate junction

Xing Yang(阳星), Jie Chen(陈杰), Yabin Yu(余亚斌), Quanhui Liu(刘全慧)
Chin. Phys. B, 2019, 28 (**9**): 097401. DOI: 10.1088/1674-1056/ab33f4

Electron transport in Dirac and Weyl semimetals

Huichao Wang(王慧超), Jian Wang(王健)
Chin. Phys. B, 2018, 27 (**10**): 107402. DOI: 10.1088/1674-1056/27/10/107402

RAPID COMMUNICATION

Josephson current in an irradiated Weyl semimetal junction*

Han Wang(王含)[1] and Rui Shen(沈瑞)[2,†]

[1] National Laboratory of Solid State Microstructures and School of Physics, Nanjing University, Nanjing 210093, China
[2] Collaborative Innovation Center of Advanced Microstructures, Nanjing University, Nanjing 210093, China

(Received 7 April 2021; revised manuscript received 9 May 2021; accepted manuscript online 20 May 2021)

The influence of the off-resonant circularly polarized light on the Josephson current in the time-reversal broken superconducting Weyl semimetal junctions is investigated by using the Bogoliubov–de Gennes equation and the transfer matrix approach. Both the zero momentum BCS pairing states and the finite momentum Fulde–Ferrell–Larkin–Ovchinnikov (FFLO) pairing states are considered for the Weyl superconductors. When a circularly polarized light is applied, it is shown that the current phase relation remains unchanged for the BCS pairing with the increasing of incident radiation intensity A_0. For FFLO pairing, the Josephson current exhibits the 0–π transition and periodic oscillation as a function of A_0. The dependence of free energy and critical current on A_0 are also investigated.

Keywords: Weyl semimetal, Josephson junction, FFLO pairing

PACS: 73.23.–b, 74.20.–z, 74.50.+r **DOI:** 10.1088/1674-1056/ac0348

1. Introduction

The Weyl semimetal is a three-dimensional topological material, where the conduction band and the valance band touch each other at two or more Weyl nodes and the paired Weyl nodes are connected by the unusual Fermi arcs.[1–7] The low-energy physics of the electrons around the Weyl node can be effectively described by the Weyl equation. Due to the no-go theorem,[8] the Weyl nodes always come in pairs with opposite chiralities. In order to realize the Weyl semimetal phase, the time reversal symmetry or the inversion symmetry are required to be broken.[9–11]

There are many interesting properties of the Weyl semimetals, such as the negative magnetoressitance,[12] the chiral anomaly,[13] and the anomalous Hall effect.[14,15] The superconducting pairing mechanism in the Weyl semimetals has also attracted much attention.[16–20] Two competing pairing states have been proposed, *i.e.*, the internode BCS pairing and the intranode Fulde–Ferrell–Larkin–Ovchinnikov (FFLO) pairing. The internode pairing combines two electrons from two Weyl cones of opposite chiralities and leads to the Cooper pair with zero-momentum. The intanode pairing combines two electrons from the same Weyl cone and leads to the Cooper pair with a finite momentum. It still remains a theoretical controversy that which pairing mechanism is favored in energy.[17,20]

Josephson current can be an effective method to probe the superconducting pairing mechanism.[21–31] Recently, there are several works focus on the Josephson effect and superconducting pairing mechanisms based on Weyl semimetal superconductor heterostructures. The influence of the chiral anomaly induced chiral charge imbalance on the Josephson current in a Weyl superconductor–Weyl semimetal–Weyl superconductor junction has been theoretically studied.[31] For BCS-like pairing, it has been predicted that the Josephson current exhibits 0–π transitions and oscillates as a function of chirality imbalance. It has also been predicted[32] that inversion symmetric tilt will induce 0–π transition and Josephson φ_0 junction in BCS-like pairing.

In this paper, we investigate the dc Josephson current in the time-reversal broken superconducting Weyl semimetal junctions. A circularly polarized light is applied in the normal region of the junction and leads to an additional momentum shift to the electrons at the Fermi level. The momentum shifts are opposite for the electrons of the opposite chiralities. As a result, it is shown that the current phase relation remains unchanged for the BCS pairing and exhibits the 0–π transition for the FFLO pairing, respectively. The different signals of the Josephson currents in the optical field may obtain a way to distinguish between the internode and intranode pairing cases.

The rest of this paper is organized as follows: our model is described in Section 2. The Andreev bound states and the Josephson current are obtained analytically in Section 3. The numerical results of the Josephson current are discussed in Section 4. Finally, our results are briefly concluded in Section 5.

2. Model

The time-reversal broken Weyl semimetal junction under consideration is a normal Weyl semimetal sandwiched be-

*Project supported by the National Key Research and Development Program of China (Grant No. 2017YFA0303203) and the National Natural Science Foundation of China (Grant No. 11474149).

†Corresponding author. E-mail: shen@nju.edu.cn

© 2021 Chinese Physical Society and IOP Publishing Ltd

tween two superconducing Weyl semimetal leads, as shown in Fig. 1(a). The junction is along the z axis and the width of the normal segment is d. There are at least one pair of Weyl nodes, namely $\boldsymbol{P}_{\pm} = \pm\boldsymbol{P}_0$, located in the momentum space. The line connecting $\boldsymbol{P}_{\pm}$ (axis e_3) is assumed in the x–z plane but has an angle β with the z axis, as shown in Fig. 1(b).

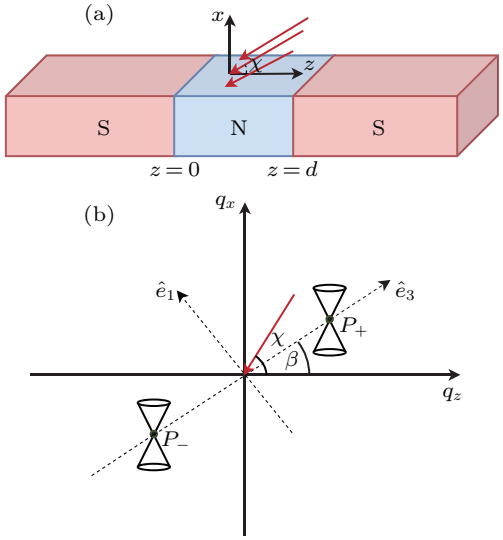


Fig. 1. (a) Schematic diagram of the Josephson junction. An irradiated Weyl semimetal with the incident light denoted by red arrows is sandwiched between two superconducting Weyl semimetals. The interfaces are at $z = 0$ and $z = d$, respectively. (b) The illustration of the x–z coordinates and the e_1–e_3 coordinates. The line connecting two Weyl nodes (the e_3 axis) is rotated from the z axis by an angle β. The direction of the optical field is measured from the z axis by an azimuth angle χ.

The minimal model of the Weyl semimetal without optical field is described by an effective two-band Hamiltonian, which is written in the e_1–e_3 coordinates as[33]

$$\begin{aligned} H &= \sum_{\tau=\pm}\sum_{\boldsymbol{q}} \Psi^{\dagger}_{\tau\boldsymbol{q}} H_{\tau}(\boldsymbol{q}) \Psi_{\tau\boldsymbol{q}}, \\ H_{\pm}(\boldsymbol{q}) &= \hbar v_{\mathrm{F}}(q_1\sigma_1 + q_2\sigma_2 \mp q_3\sigma_3) - \mu, \end{aligned} \tag{1}$$

where $\tau = \pm$ denotes the chirality of two Weyl nodes, $\boldsymbol{q}$ is the momentum measured from the Weyl node, v_{F} is the Fermi velocity, $\boldsymbol{\sigma}$ is the Pauli matrix, and $\Psi^{\dagger}_{\tau\boldsymbol{q}} = \left(c^{\dagger}_{\tau,\uparrow,\boldsymbol{q}}, c^{\dagger}_{\tau,\downarrow,\boldsymbol{q}}\right)$ is the field operator of the electrons.

An incident light in x–z plane can be expressed by its vector potential

$$\boldsymbol{A}(t) = (A_x\cos(\omega t), A_y\sin(\omega t + \delta), A_z\cos(\omega t)) \tag{2}$$

with $A_x = E_0\cos\chi, A_y = E_0, A_z = -E_0\sin\chi$ where ω and E_0 are the frequency and the amplitude of the optical field, respectively, χ is the the azimuth angle between the incident light and the z axis, δ represents light polarization and $\delta = 0$ (π) represents the right (left)-hand circularly polarized light. In the presence of optical light, the time-dependent Hamiltonian can be described by Peierls substitution $H(\boldsymbol{q},t) = H(\boldsymbol{q} + e\boldsymbol{A}(t)/\hbar)$. Here we focus on the high driving frequency ω greater than the static energy bandwidth, so that an effective Hamiltonian reads[34–38]

$$H_{\mathrm{eff}}(\boldsymbol{q}) = H_0(\boldsymbol{q}) + \sum_{n>0}\frac{[H_n(\boldsymbol{q}), H_{-n}(\boldsymbol{q})]}{n\omega} + \hat{O}\left(\frac{1}{\omega^2}\right), \tag{3}$$

where $H_n(\boldsymbol{q}) = \frac{1}{T}\int_{-T/2}^{T/2} \mathrm{d}t H(\boldsymbol{q},t)\,\mathrm{e}^{-\mathrm{i}n\omega t}$ is the Fourier component of the time-dependent Hamiltonian with period $T = 2\pi/\omega$. We define a rotation matrix to associate the x–z coordinates with the $\boldsymbol{e}_1$–$\boldsymbol{e}_3$ coordinates, which reads

$$\begin{aligned} \hat{R} &= \begin{pmatrix} \cos\beta & 0 & -\sin\beta \\ 0 & 1 & 0 \\ \sin\beta & 0 & \cos\beta \end{pmatrix}, \\ (q_1, q_2, q_3)^{\mathrm{T}} &= \hat{R}(q_x, q_y, q_z)^{\mathrm{T}}, \\ (\sigma_1, \sigma_2, \sigma_3)^{\mathrm{T}} &= \hat{R}(\sigma_x, \sigma_y, \sigma_z)^{\mathrm{T}}. \end{aligned} \tag{4}$$

The full time-dependent Hamiltonian can be expressed as

$$\begin{aligned} H_{\pm}(\boldsymbol{q},t) &= H_{\pm}(\boldsymbol{q}) + \mathcal{V}_{\pm}(t), \\ \mathcal{V}_{\pm}(t) &= ev_{\mathrm{F}}E_0(\cos\omega t\cos(\beta-\chi)\sigma_1 \\ &\quad \mp\cos\omega t\sin(\beta-\chi)\sigma_3 + \sin(\omega t+\delta)\sigma_2). \end{aligned} \tag{5}$$

By using the Floquet theory, the effective Hamiltonian of irradiated Weyl semimetal can be described as

$$\begin{aligned} H^{\mathrm{eff}}_{\pm}(\boldsymbol{q}) &= \hbar v_{\mathrm{F}}[(q_1 \mp A_0\cos\delta\sin(\beta-\chi))\sigma_1 + q_2\sigma_2 \\ &\quad \mp(q_3 \pm A_0\cos\delta\cos(\beta-\chi))\sigma_3] - \mu \end{aligned} \tag{6}$$

with $A_0 = v_{\mathrm{F}}\mathrm{e}^2E_0^2/\hbar\omega$ being the circularly polarized light intensity which is only introduced in the normal region of the junction. For simplicity, we only consider the right-hand circularly polarized light ($\delta = 0$) below and we also adopt the units $\hbar v_{\mathrm{F}} = 1$ so that both the wave vector and the A_0 have the dimensionality of the energy. Due to the optical field, an electron with a given energy acquires an additional momentum shift which are opposite for electrons in the $\boldsymbol{P}_+$ and those in the $\boldsymbol{P}_-$ cones.

In the superconducting region, both the internode BCS pairing term and the intranode FFLO pairing term are considered, which can be expressed as

$$\begin{aligned} H^{\mathrm{B}}_{\mathrm{pair}} &= \sum_{\boldsymbol{q},\tau}\Delta_0 c^{\dagger}_{\tau,\uparrow,\boldsymbol{q}}c^{\dagger}_{-\tau,\downarrow,-\boldsymbol{q}} + \mathrm{h.c.}, \\ H^{\mathrm{F}}_{\mathrm{pair}} &= \sum_{\boldsymbol{q},\tau}\Delta_0 c^{\dagger}_{\tau,\uparrow,\boldsymbol{q}}c^{\dagger}_{\tau,\downarrow,-\boldsymbol{q}} + \mathrm{h.c.}, \end{aligned} \tag{7}$$

where Δ_0 is the pair potential. With the help of $q = -\mathrm{i}\boldsymbol{\nabla} - \boldsymbol{P}_{\pm}$, Hamilton (6) can be written in the spatial space. In the Nambu basis $[\psi_{\uparrow}(\boldsymbol{r}), \psi_{\downarrow}(\boldsymbol{r}), \psi^{\dagger}_{\downarrow}(\boldsymbol{r}), -\psi^{\dagger}_{\uparrow}(\boldsymbol{r})]^{\mathrm{T}}$, the Bogoliubov–de Gennes (BdG) Hamilton reads

$$\begin{aligned} H_{\mathrm{B}} &= \begin{pmatrix} H^{\mathrm{eff}}_{+}(-\mathrm{i}\boldsymbol{\nabla} - \boldsymbol{P}_0) & \Delta_0 \\ \Delta_0^* & -\mathcal{T}H^{\mathrm{eff}}_{-}(-\mathrm{i}\boldsymbol{\nabla} + \boldsymbol{P}_0)\mathcal{T}^{-1} \end{pmatrix}, \\ H^{\pm}_{\mathrm{F}} &= \begin{pmatrix} H^{\mathrm{eff}}_{\pm}(-\mathrm{i}\boldsymbol{\nabla} \mp \boldsymbol{P}_0) & \Delta_0\,\mathrm{e}^{\pm 2\mathrm{i}\boldsymbol{P}_0\cdot\boldsymbol{r}} \\ \Delta_0^*\,\mathrm{e}^{\mp 2\mathrm{i}\boldsymbol{P}_0\cdot\boldsymbol{r}} & -\mathcal{T}H^{\mathrm{eff}}_{\pm}(-\mathrm{i}\boldsymbol{\nabla} \mp \boldsymbol{P}_0)\mathcal{T}^{-1} \end{pmatrix}, \end{aligned} \tag{8}$$

where $\mathcal{T}=\mathrm{i}\sigma_2\mathcal{K}$ is the time-reversal operator with $\mathcal{K}$ being the operator of complex conjugation.

For the convenience of the calculation, one can employ a unitary transformation[39] on Hamiltonian (8) and get

$$\tilde{H}_{\mathrm{B}}=U_{\mathrm{B}}H_{\mathrm{B}}U_{\mathrm{B}}^{-1}=\begin{pmatrix}\tilde{H}_{+}(A_0)-\mu & \Delta_{\mathrm{B}}\\ \Delta_{\mathrm{B}}^{*} & \mu-\tilde{H}_{-}(-A_0)\end{pmatrix},$$
$$\tilde{H}_{\mathrm{F}}^{\pm}=U_{\mathrm{F}}^{\pm}H_{\mathrm{F}}^{\pm}(U_{\mathrm{F}}^{\pm})^{-1}=\begin{pmatrix}\tilde{H}_{\pm}(A_0)-\mu & \Delta_{\mathrm{F}}\\ \Delta_{\mathrm{F}}^{*} & \mu-\tilde{H}_{\pm}(-A_0)\end{pmatrix}, \quad (9)$$

where

$$U_{\mathrm{B}}=\frac{1}{2}[(\tau_0+\tau_z)\sigma_x\mathrm{e}^{\mathrm{i}\beta\sigma_y}+(\tau_0-\tau_z)\sigma_0]\,\mathrm{e}^{\mathrm{i}\boldsymbol{P}_0\cdot\boldsymbol{r}},$$
$$U_{\mathrm{F}}^{+}=\tau_0\sigma_x\mathrm{e}^{\mathrm{i}\beta\sigma_y}\mathrm{e}^{\mathrm{i}\tau_z\boldsymbol{P}_0\cdot\boldsymbol{r}},\quad U_{\mathrm{F}}^{-}=\mathrm{e}^{-\mathrm{i}\tau_z\boldsymbol{P}_0\cdot\boldsymbol{r}},$$
$$\Delta_{\mathrm{B}}=\Delta_0(\sigma_x\cos\beta-\sigma_z\sin\beta),\quad \Delta_{\mathrm{F}}=\Delta_0, \quad (10)$$

and $\tau_{0,x,y,z}$ are the unit and Pauli matrices acting in the particle–hole space. Hamiltonian $\tilde{H}_{\pm}$ is given by

$$\tilde{H}_{\pm}=\begin{pmatrix}-\mathrm{i}\partial_z\pm A_0\cos\chi & -\mathrm{i}\partial_x\pm A_0\sin\chi\pm\partial_y\\ -\mathrm{i}\partial_x\pm A_0\sin\chi\mp\partial_y & \mathrm{i}\partial_z\pm A_0\cos\chi\end{pmatrix}. \quad (11)$$

We note that the chemical potential and the pair potential are different in the different segments of the junction. The superconducting leads are heavily doped so that the Weyl nodes are well below the Fermi level. Therefore, the density of states at the Fermi level in the superconductor is large enough to form the condensation. While in the normal segment, the chemical potential remains finite and, in the rest of this paper, we use μ_{N} to denote the Fermi energy measured from the Weyl nodes in the normal region. We adopt the step approximation for the pair potential, which is assumed zero in the normal region and finite in the superconductors. A macroscopic phase of $\pm\varphi/2$ is assigned to the pair potentials in the right and left superconductors, respectively.

3. Andreev bound state

Based on the transfer matrix formalism, the Andreev bound states and the Josephson current can be obtained.[40] Taking the BCS pairing case as an example, the eigenwavefunction of the BdG Hamiltonian (9) for quasiparticles of energy ε in the left superconductor reads

$$\Psi_{\mathrm{L1}}^{\mathrm{S}}(z)=\left(-\mathrm{e}^{-\mathrm{i}\gamma_{\mathrm{B}}},0,\mathrm{e}^{\mathrm{i}\varphi/2},0\right)^{\mathrm{T}}\mathrm{e}^{\mathrm{i}q_{\mathrm{F}}z+\kappa_{\mathrm{B}}z},$$
$$\Psi_{\mathrm{L2}}^{\mathrm{S}}(z)=\left(0,\mathrm{e}^{\mathrm{i}\gamma_{\mathrm{B}}},0,\mathrm{e}^{\mathrm{i}\varphi/2}\right)^{\mathrm{T}}\mathrm{e}^{-\mathrm{i}q_{\mathrm{F}}z+\kappa_{\mathrm{B}}z}, \quad (12)$$

where

$$\gamma_{\mathrm{B}}=\arccos\frac{\varepsilon}{\Delta_0\sin\beta},\quad \kappa_{\mathrm{B}}=\sqrt{\Delta_0^2\sin^2\beta-\varepsilon^2}, \quad (13)$$

and q_{F} is the Fermi wave vector in the superconductor. The wave vectors are properly chosen so that the wave functions decays exponentially in the infinity. Each four-component wave function can be divided into two parts, the first two components called $\Psi_{\mathrm{e}}^{\mathrm{S}}$ and the last two components called $\Psi_{\mathrm{h}}^{\mathrm{S}}$. At the boundary, $\Psi_{\mathrm{e}}^{\mathrm{S}}$ and $\Psi_{\mathrm{h}}^{\mathrm{S}}$ are related by the transfer matrix given by

$$\Psi_{\mathrm{h}}^{\mathrm{S}}(z=0)=U_{\mathrm{L}}\Psi_{\mathrm{e}}^{\mathrm{S}}(z=d),$$
$$U_{\mathrm{L}}=-\sigma_z\mathrm{e}^{\mathrm{i}\varphi/2+i\gamma_{\mathrm{B}}\sigma_z}. \quad (14)$$

In the right superconductor, one can similarly find that

$$\Psi_{\mathrm{R1}}^{\mathrm{S}}(z)=\left(-\mathrm{e}^{\mathrm{i}\gamma_{\mathrm{B}}},0,\mathrm{e}^{-\mathrm{i}\varphi/2},0\right)^{\mathrm{T}}\mathrm{e}^{\mathrm{i}q_{\mathrm{F}}z-\kappa_{\mathrm{B}}z},$$
$$\Psi_{\mathrm{R2}}^{\mathrm{S}}(z)=\left(0,\mathrm{e}^{-\mathrm{i}\gamma_{\mathrm{B}}},0,\mathrm{e}^{-\mathrm{i}\varphi/2}\right)^{\mathrm{T}}\mathrm{e}^{-\mathrm{i}q_{\mathrm{F}}z-\kappa_{\mathrm{B}}z}, \quad (15)$$
$$\Psi_{\mathrm{h}}^{\mathrm{S}}(z=d)=U_{\mathrm{R}}\Psi_{\mathrm{e}}^{\mathrm{S}}(z=d),$$
$$U_{\mathrm{R}}=-\sigma_z\mathrm{e}^{-\mathrm{i}\varphi/2-i\gamma_{\mathrm{B}}\sigma_z}. \quad (16)$$

In the normal region, we have four wave functions representing the leftgoing and the rightgoing electrons and holes, respectively, which are written as

$$\Psi_{\overrightarrow{e}}(z)=\left(\cos\alpha_{\mathrm{e}}/2,\mathrm{e}^{-\mathrm{i}\theta_{\mathrm{e}}}\sin\alpha_{\mathrm{e}}/2,0,0\right)^{\mathrm{T}}\mathrm{e}^{\mathrm{i}q_{z,\overrightarrow{e}}z},$$
$$\Psi_{\overleftarrow{e}}(z)=\left(\mathrm{e}^{\mathrm{i}\theta_{\mathrm{e}}}\sin\alpha_{\mathrm{e}}/2,\cos\alpha_{\mathrm{e}}/2,0,0\right)^{\mathrm{T}}\mathrm{e}^{\mathrm{i}q_{z,\overleftarrow{e}}z},$$
$$\Psi_{\overleftarrow{h}}(z)=\left(0,0,\cos\alpha_{\mathrm{h}}/2,\mathrm{e}^{\mathrm{i}\theta_{\mathrm{h}}}\sin\alpha_{\mathrm{h}}/2\right)^{\mathrm{T}}\mathrm{e}^{\mathrm{i}q_{z,\overleftarrow{h}}z},$$
$$\Psi_{\overrightarrow{h}}(z)=\left(0,0,\mathrm{e}^{-\mathrm{i}\theta_{\mathrm{h}}}\sin\alpha_{\mathrm{h}}/2,\cos\alpha_{\mathrm{h}}/2\right)^{\mathrm{T}}\mathrm{e}^{\mathrm{i}q_{z,\overrightarrow{h}}z}, \quad (17)$$

where the angles

$$\theta_{\mathrm{e(h)}}=\arcsin\frac{q_y}{q_{\parallel,e(h)}},\quad \alpha_{\mathrm{e(h)}}=\arctan\frac{q_{\parallel,e(h)}}{q_{z,e(h)}}, \quad (18)$$

and the wavevectors

$$q_{\parallel,e(h)}=\sqrt{(q_x+A_0\sin\chi)^2+q_y^2},$$
$$q_{z,\overrightarrow{e}}=-A_0\cos\chi+q_{z,e},\quad q_{z,\overleftarrow{e}}=-A_0\cos\chi-q_{z,e},$$
$$q_{z,\overleftarrow{h}}=-A_0\cos\chi+q_{z,h},\quad q_{z,\overrightarrow{h}}=-A_0\cos\chi-q_{z,h},$$
$$q_{z,e(h)}=\sqrt{(\varepsilon\pm\mu_N)^2-q_{\parallel,e(h)}^2}. \quad (19)$$

As the case in the superconducting leads, the four-component wave functions in the normal region can also be divided into two-component wave functions Ψ_{e} and Ψ_{h}, which are connected at the boundaries as

$$\Psi_{\mathrm{e}}(z=d)=M_{\mathrm{e}}\Psi_{\mathrm{e}}(z=0),$$
$$\Psi_{\mathrm{h}}(z=d)=M_{\mathrm{h}}\Psi_{\mathrm{h}}(z=0), \quad (20)$$

with the transfer matrices

$$M_{\mathrm{e}}=\Lambda_{\mathrm{e}}\mathrm{e}^{\mathrm{i}q_{z,e}d\sigma_z-A_0\cos\chi d\sigma_0}\Lambda_{\mathrm{e}}^{-1},$$
$$M_{\mathrm{h}}=\Lambda_{\mathrm{h}}\mathrm{e}^{\mathrm{i}q_{z,h}d\sigma_z-A_0\cos\chi d\sigma_0}\Lambda_{\mathrm{h}}^{-1}, \quad (21)$$
$$\Lambda_{\mathrm{e}}=\begin{pmatrix}\cos(\alpha_{\mathrm{e}}/2) & \mathrm{e}^{\mathrm{i}\theta_{\mathrm{e}}}\sin(\alpha_{\mathrm{e}}/2)\\ \mathrm{e}^{-\mathrm{i}\theta_{\mathrm{e}}}\sin(\alpha_{\mathrm{e}}/2) & \cos(\alpha_{\mathrm{e}}/2)\end{pmatrix}, \quad (22)$$
$$\Lambda_{\mathrm{h}}=\begin{pmatrix}\cos(\alpha_{\mathrm{h}}/2) & \mathrm{e}^{-\mathrm{i}\theta_{\mathrm{h}}}\sin(\alpha_{\mathrm{h}}/2)\\ \mathrm{e}^{\mathrm{i}\theta_{\mathrm{h}}}\sin(\alpha_{\mathrm{h}}/2) & \cos(\alpha_{\mathrm{h}}/2)\end{pmatrix}. \quad (23)$$

The continuity of the wave functions at the boundaries results in

$$\mathrm{Det}\left(1-M_{\mathrm{e}}^{-1}U_{\mathrm{R}}^{-1}M_{\mathrm{h}}U_{\mathrm{L}}\right)=0, \tag{24}$$

which gives the Andreev bound energies.[40] For the short junction of $d \ll \xi$ with the superconducting coherent length $\xi \sim \hbar v_{\mathrm{F}}/\Delta_0$, one usually adopts the approximation $\Delta_0 \ll \mu_N$. Thus the energy dependence in angles $\alpha_{\mathrm{e,h}}$ and $\theta_{\mathrm{e,h}}$ can be neglected[40] and the Andreev bound energy is obtained analytically as

$$\left(\frac{\varepsilon_{\mathrm{B}}}{\Delta_0\sin\beta}\right)^2 = \frac{1}{2}\left\{1+\frac{A[C+\cos\varphi]}{A^2+B^2} \pm\sqrt{\frac{B^2}{(A+B)^2}\left(A^2+B^2-[C+\cos\varphi]^2\right)}\right\}, \tag{25}$$

where

$$\begin{aligned} A &= \cos q_{z,e}d\cos q_{z,h}d+\frac{\sin q_{z,e}d\sin q_{z,h}d}{\cos\alpha_{\mathrm{e}}\cos\alpha_{\mathrm{h}}},\\ B &= \frac{\sin q_{z,e}d\cos q_{z,h}d}{\cos\alpha_{\mathrm{e}}}-\frac{\cos q_{z,e}d\sin q_{z,h}d}{\cos\alpha_{\mathrm{h}}},\\ C &= \cos(\theta_{\mathrm{e}}+\theta_{\mathrm{h}})\sin q_{z,e}d\sin q_{z,h}d\tan\alpha_{\mathrm{e}}\tan\alpha_{\mathrm{h}}. \end{aligned} \tag{26}$$

The Andreev bound energies in the FFLO pairing case can be obtained similarly. In contrast to the internode BCS pairing, the condensation in the FFLO case occurs in each Weyl cone independently. Therefore, the Andreev bound energies for the two Weyl nodes are different, which are written as

$$\begin{aligned} &\left(\frac{\varepsilon_{\mathrm{F}\pm}}{\Delta_0}\right)^2\\ &= \frac{1}{2}\left\{1+\frac{A[F+\cos(\varphi-2\varphi_{\mathrm{F}\pm})]}{A^2+B^2}\right.\\ &\left.\pm\sqrt{\frac{B^2}{(A+B)^2}\left(A^2+B^2-[F+\cos(\varphi-2\varphi_{\mathrm{F}\pm})]^2\right)}\right\}, \end{aligned} \tag{27}$$

with

$$\begin{aligned} \varphi_{\mathrm{F}\pm} &= \pm\varphi_{\mathrm{F}} = \pm A_0 d\cos\chi,\\ F &= \cos(\theta_{\mathrm{e}}-\theta_{\mathrm{h}})\sin q_{z,e}d\sin q_{z,h}d\tan\alpha_{\mathrm{e}}\tan\alpha_{\mathrm{h}}. \end{aligned} \tag{28}$$

We note that the expression for the $q_{\parallel,e(h)}$ in the FFLO case is different from that in the BCS case (Eq. (19)). One obtains

$$q_{\parallel,e(h)} = \sqrt{(q_x \pm A_0\sin\chi)^2+q_y^2}, \tag{29}$$

for the calculation of $\varepsilon_{\mathrm{F}+}$ and

$$q_{\parallel,e(h)} = \sqrt{(q_x \mp A_0\sin\chi)^2+q_y^2}, \tag{30}$$

for the calculation of $\varepsilon_{\mathrm{F}-}$, respectively.

With the help of the Andreev bound energies, the free energy of the junction is given by[41–43]

$$F = -2k_{\mathrm{B}}T\sum_{q_x,q_y}\sum_{b}\ln[2\cosh(\varepsilon_b/2k_{\mathrm{B}}T)]+F_0, \tag{31}$$

where ε_b is the Andreev bound energy defined in Eqs. (25) and (27), the summation over b is restricted to all positive Andreev bound energies, and F_0 is a term independent of the phase difference φ. Under the short junction approximation, only the contribution from the Andreev bound states is taken into account and that from the continuous spectrum is neglected in Eq. (31).[41–43] Finally, the Josephson current can be obtained as[41]

$$I(\varphi) = -\frac{2e}{\hbar}\sum_{q_x,q_y}\sum_{b}\frac{\partial\varepsilon_b}{\partial\varphi}\tanh(\varepsilon_b/2k_{\mathrm{B}}T). \tag{32}$$

It is easy to find that the Josphson current for BCS-like pairing reads

$$I_{\mathrm{B}} \sim (I_+ + I_-)\sin\varphi \sim 2I_0\sin\varphi, \tag{33}$$

while for FFLO-like pairing, the Josephson current is given by

$$I_{\mathrm{F}} \sim I_+\sin(\varphi-2\varphi_{\mathrm{F}})+I_-\sin(\varphi+2\varphi_{\mathrm{F}}), \tag{34}$$

where I_+ and I_- are the current contributions from the two Weyl cones of opposite chiralities.

4. Results

First, we briefly discuss the basic concepts and the qualitative results on the Andreev bound states under the Bohr–Sommerfield quantization condition.[44,45] This will be very helpful in understanding the numerical results provided later. According to the Bohr–Sommerfield quantization condition, the Andreev bound state is determined by $\oint p\,\mathrm{d}z+\varphi_{\mathrm{A}} = 2n\pi$, where φ_{A} is the total phase shift obtained by the Andreev reflections and $\oint p\,\mathrm{d}z$ is the phase shift accumulated by the quasiparticle moving in a loop in the normal region between two interfaces at $z=0$ and $z=d$, respectively. Under the circularly polarized light, the quasiparticle at the Fermi level acquires an additional momentum shift which results in an addition phase in $\oint p\,\mathrm{d}z$ and the phase dependence of the Andreev bound energy.

In the BCS pairing case, the Cooper pair is composed by two electrons from the Weyl cones of opposite chiralities. From Eq. (6) one finds that the momentum shifts for the electrons in the two Weyl cones are opposite, namely, $\pm A_0\cos(\chi)$, respectively. The loop phase contains the contributions from a rightgoing electron and a leftgoing hole, which can be treated as the phase shift from two rightgoing electrons. Since the two electrons are from different Weyl cones and acquire the opposite phase shifts, the loop phase shift remains unchanged. Therefore, the phase dependence of the Andreev bound energy and the current phase relation of the Josephson junction remain unchanged.

In the FFLO pairing case, the Cooper pair is composed by two electrons of the same chirality. The accumulated phase shift of the rightgoing electron and that of the leftgoing hole in a loop are always the same. However, the total phase shift in a loop in the P_+ cone and that in the P_- cone may be different. The phase shifts in a loop in the P_+ cone is $2\varphi_{F+} = 2A_0 d\cos\chi$, while that in the P_- cone is $2\varphi_{F-} = -2A_0 d\cos\chi$. The Josephson current includes the contributions from two Weyl cones, which take the form $\sin(\varphi - 2A_0 d\cos\chi)$ and $\sin(\varphi + 2A_0 d\cos\chi)$, respectively. Thus, the total current takes the form $\cos(2A_0 d\cos\chi)\sin\varphi$. As $\cos(2A_0 d\cos\chi)$ varying from positive to negative, the 0–π transition occurs. As a result, the 0–π transition can be expected in the FFLO pairing case with $\chi \neq \pi/2$.

Next, we give the numerical results of the Josephson current. The current phase relation in the BCS pairing Josephson junction is plotted in Fig. 2. The current is calculated at the temperature $T = 0.1T_c$ with T_c the superconducting transition temperature and at the width of the normal region $d/\xi = 0.025\pi$ with ξ the superconducting coherent length. The current is normalized by $J_0 = (e\Delta_0/\hbar)\cdot(\mu_N^2 S)$, where S is the section area and μ_N^2 represents the density of states at the Fermi level. When $\chi = 0$, it is shown in Fig. 2 that the junction is always a 0 junction, as analyzed by the Bohr–Sommerfield quantization condition. Moreover, one finds that the Josephson currents with different optical field strengths coincide exactly. This is due to the widely adopted approximation that the energy dependences in angles $\alpha_{e,h}$ and $\theta_{e,h}$ can be neglected in short junctions.[40,46–49] Under this approximation, from Eq. (19), one finds that the wave vectors $q_{\parallel,e} = q_{\parallel,h}$ and consequently the angles for electrons (α_e and θ_e) are exactly the same as those for holes (α_h and θ_h) when $\chi = 0$. The summation over the wave vectors in Eq. (32) is transformed into the integration over the angles α_e and θ_e and the A_0-dependence in the current vanishes.

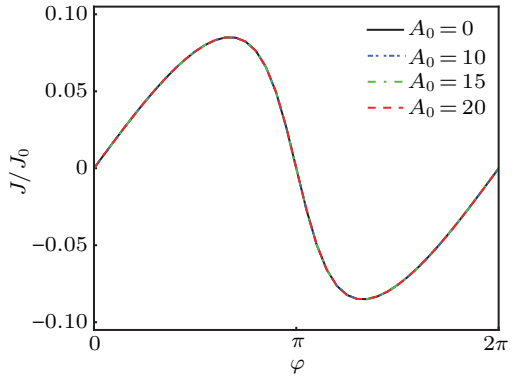


Fig. 2. Current phase relation in the BCS pairing Josephson junction. The parameters are assumed as $\mu_N = 200\Delta_0$ and $\beta = \pi/4$. The azimuth of the optical field is $\chi = 0$.

The current phase relation in the FFLO pairing Josephson junction is plotted in Fig 3. When $\chi = 0$, it is shown in Fig. 3 that the junction undergoes a 0–π transition with increasing the optical field. The Josephson current presents a standard sinusoidal curve when $A_0 = n\pi/(d\cos\chi)$ as shown by the black line in Fig. 3 which is a 0-junction. When $A_0 = (2n+1)\pi/(2d\cos\chi)$, the current-phase relation is a negative sinusoidal curve as shown by the red line which is a π-junction. Increasing A_0 from $n\pi/(d\cos\chi)$ to $(2n+1)\pi/(2d\cos\chi)$, the current phase relationship deviates from the standard sinusoidal curve with an extra zero point other than 0 or π, exhibiting a combined effect of two opposite Josephson φ_0 junction contributing from two Weyl cones as described by the Andreev bound states in Eq. (27). Especially when $A_0 = (n+1/2)\pi/(2d\cos\chi)$, the current-phase relationship changes from $\sin\varphi$ to $\sin 2\varphi$.

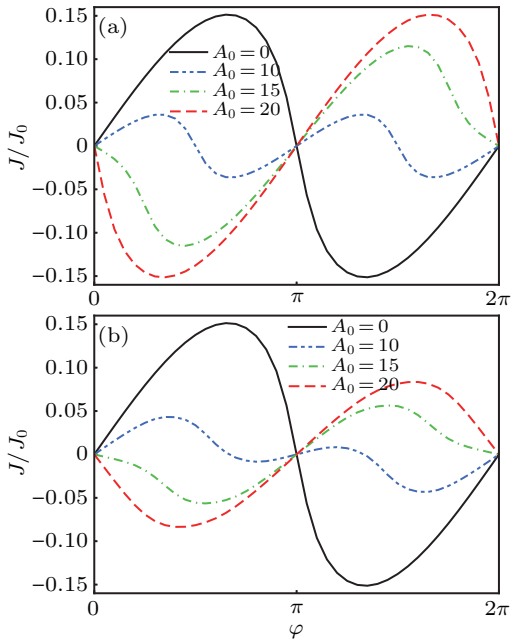


Fig. 3. Current phase relation in the FFLO pairing Josephson junction. The parameters are assumed as $\mu_N = 200\Delta_0$ and $\beta = \pi/4$. The azimuth of the optical field is $\chi = 0$ for (a), $\chi = \pi/6$ for (b), respectively.

In order to demonstrate the 0–π transition more clearly, we also plot the free energy as a function of the optical field in Fig. 4. One can easily find that, the minimum values of free energy changes with increasing optical field strength. Increasing $A_0 \sim (n+1/2)\pi/(2d\cos\chi)$,there are another dip/peak of free energy corresponding to extra zero points of the current-phase relationship. The relationship between the critical current and A_0 is plotted in Fig. 5. When $\chi = 0$, there is a dip or some dips in the A_0-dependence of the critical current as the signal of the 0–π transition. When $\chi \neq 0$, a similar behavior can be found and the critical current also decreases monotonically with the optical field.

Although our calculations are carried out with large μ_N, the main results are still valid in the regime of small μ_N. In the latter case the transport in the normal region is dominated by the evanescent modes. As a result, both J and J_0 decrease but the current phase relation remains qualitatively unchanged.[30]

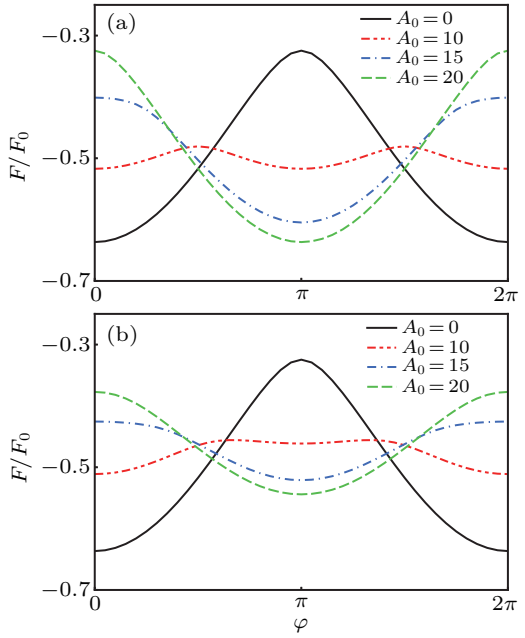


Fig. 4. The free energy is plotted as a function of phase in the FFLO pairing Josephson junction. The parameters are assumed as $\mu_N = 200\Delta_0$ and $\beta = \pi/4$. The azimuth of the optical field is $\chi = 0$ for (a), $\chi = \pi/6$ for (b), respectively.

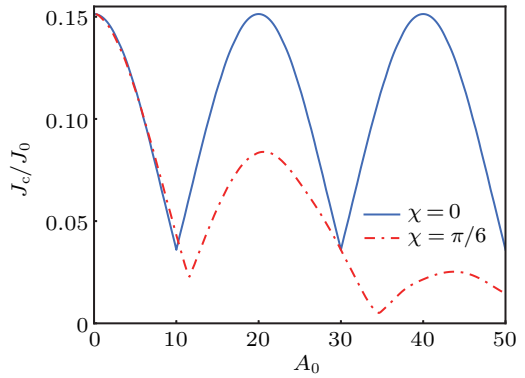


Fig. 5. The critical current is plotted as a function of A_0 in the FFLO pairing Josephson junction. The parameters are assumed as $\mu_N = 200\Delta_0$ and $\beta = \pi/4$.

5. Conclusion

In this paper, we have investigated the Josephson current in an irradiated Weyl semimetal junction. Both the internode BCS pairing and the intranode FFLO pairing are considered. The circularly polarized light-induced additional momentum shift modifies addition phase of the Andreev bound energy and the current-phase relation. It is shown that the circularly polarized light field will not alter the current phase relation for the BCS junction but can lead to a 0–π transition for the FFLO junction. The 0–π transition can only be observed for the FFLO junction and can be treated as an efficient signal for detecting the FFLO pairing in Weyl semimetals.

References

[1] Wan X G, Turner A M, Vishwanath A and Savrasov S Y 2011 *Phys. Rev. B* **83** 205101
[2] Burkov A A and Balents L 2011 *Phys. Rev. Lett.* **107** 127205
[3] Halász G B and Balents L 2012 *Phys. Rev. B* **85** 035103
[4] Zyuzin A A, Wu S and Burkov A A 2012 *Phys. Rev. B* **85** 165110
[5] Burkov A A 2016 *Nat. Mater.* **15** 1145
[6] Wang H C and Wang J 2018 *Chin. Phys. B* **27** 107402
[7] Armitage N P, Mele E J and Vishwanath A 2018 *Rev. Mod. Phys.* **90** 015001
[8] Nielsen H B and Ninomiya M 1981 *Phys. Lett. B* **105** 219
[9] Yang K Y, Lu Y M and Ran Y 2011 *Phys. Rev. B* **84** 075129
[10] Turner A M and Vishwanath A 2013 arXiv:1301.0330 [cond-mat.str-el]
[11] Lv B Q, Weng H M, Fu B B, Wang X P, Miao H, Ma J, Richard P, Huang X C, Zhao L X, Chen G F, Fang Z, Dai X, Qian T and Ding H 2015 *Phys. Rev. X* **5** 031013
[12] Son D T and Spivak B Z 2013*Phys. Rev. B* **88** 104412
[13] Ashby P E C and Carbotte J P 2014*Phys. Rev. B* **89** 245121
[14] Burkov A A 2014 *Phys. Rev. Lett.* **113** 187202
[15] Wang G Q, Sun Z H, Si X and Jia S 2020 *Chin. Phys. B* **29** 077503
[16] Meng T and Balents L 2012 *Phys. Rev. B* **86** 054504
[17] Cho G Y, Bardarson J H, Lu Y M and Moore J E 2012 *Phys. Rev. B* **86** 214514
[18] Das T 2013 *Phys. Rev. B* **88** 035444
[19] Bednik G, Zyuzin A A and Burkov A A 2015 *Phys. Rev. B* **92** 035153
[20] Zhou T, Gao Y and Wang Z D 2016 *Phys. Rev. B* **93** 094517
[21] Tanaka Y, Golubov A A, Kashiwaya S and Masahito U 2007 *Phys. Rev. Lett.* **99** 037005
[22] Wu W X, Feng Y, Bai Y H, Jiang Y Y, Gao Z W, Li Y Z, Luan J L, Zhou H A, Jiang W J, Feng X, Zhang J S, Zhang H, He K, Ma X C, Xue Q K and Wang Y Y 2021 *Chin. Phys. Lett.* **38** 037402
[23] Linder J, Yokoyama T and Sudbø A 2008 *Phys. Rev. B* **77** 174507
[24] Linder J, Sperstad I B and Sudbø A 2009 *Phys. Rev. B* **80** 020503
[25] Wang D, Lu H Y and Wang Q H 2013 *Chin. Phys. Lett.* **30** 077404
[26] Wu B H, Feng X Y, Wang C, Xu X F and Wang C R 2016 *Chin. Phys. Lett.* **33** 017401
[27] Zeng W and Shen R 2018 *Chin. Phys. B* **27** 097401
[28] Kalenyuk A A, Pagliero A, Borodianskyi E A, Kordyuk A A and Krasnov V M 2018 *Phys. Rev. Lett.* **120** 067001
[29] Bauer A G and Sothmann B 2019 *Phys. Rev. B* **99** ,214508
[30] Madsen K A, Bergholtz E J and Brouwer P W 2017 *Phys. Rev. B* **95** 064511
[31] Uddin S, Duan W Y, Wang J, Ma Z S and Liu J F 2019 *Phys. Rev. B* **99** 045426
[32] Sinha D 2020 *Phys. Rev. B* **102** 085144
[33] Chen W, Jiang L, Shen R, Sheng L, Wang B G and Xing D Y 2013 *Europhys. Lett.* **103** 27006
[34] Wang R, Wang B G, Shen R, Sheng L and Xing D Y 2014 *Europhys. Lett.* **105** 17004
[35] Khanna U, Rao S and Kundu A 2017 *Phys. Rev. B* **95** 201115
[36] Menon A, Chowdhury D and Basu B 2018 *Phys. Rev. B* **98** 205109
[37] Fu P H, Wang J, Liu J F and Wang R Q 2019 *Phys. Rev. B* **100** 115414
[38] Li X S, Wang C, Deng M X, Duan H J, Fu P H, Wang R Q, Sheng L and Xing D Y 2019 *Phys. Rev. Lett.* **123** 206601
[39] Breunig D, Zhang S B, Stehno M and Trauzettel B 2019 *Phys. Rev. B* **99** 174501
[40] Titov M and Beenakker C W J 2006 *Phys. Rev. B* **74** 041401
[41] Beenakker C W J 1991 *Phys. Rev. Lett.* **67** 3836
[42] Annunziata G, Enoksen H, Linder J, Cuoco M, Noce C and Sudbø A 2011 *Phys. Rev. B* **83** 144520
[43] Zhou X F and Jin G J 2017 *Phys. Rev. B* **95** 195419
[44] Bagwell P F 1992 *Phys. Rev. B* **46** 12573
[45] Zagoskin A M 1998 *Quantum theory of many-body systems* (New York: Springer) pp. 204–206
[46] Nussbaum J, Schmidt T L, Bruder C and Tiwari R P 2014 *Phys. Rev. B* **90** 045413
[47] Li H, Wang R and Ting C S 2016 *Phys. Rev. B* **94** 085422
[48] Linder J and Yokoyama T 2014 *Phys. Rev. B* **89** 020504
[49] Linder J, Tanaka Y, Yokoyama T, Sudbø A and Nagaosa N 2010 *Phys. Rev. B* **81** 184525